# Calculation of Carbon Ablation on a Re-Entry Body During Supersonic/Subsonic Flight

L.W. Hunter,* L.L. Perini,† D.W. Conn,‡ and P.T. Brenza§
*The John Hopkins University/Applied Physics Laboratory, Laurel, Maryland*

**A simplified but accurate procedure for calculating carbon recession and temperature histories of re-entry bodies designed to slow down to subsonic speeds before impact is presented. The method accounts for finite rate chemistry and predicts results substantially different from diffusion-limited ablation calculations.**

## Nomenclature

$A$ = pre-exponential factor
$B$ = mass-transfer parameter
$D$ = diffusivity
$Da$ = Damköhler number
$E$ = activation temperature
$g$ = mass-transfer conductance
$g^*$ = mass transfer conductance, no blowing
$i$ = enthalpy per unit mass
$\Delta\bar{i}$ = change in partial molar enthalpy
$I$ = incident radiation flux
$k$ = reaction rate coefficient
$m$ = mass fraction
$M$ = molecular weight
$\ddot{q}''$ = in-depth heat flux
$y$ = distance from surface
$\epsilon$ = emissivity
$\rho$ = density
$\sigma$ = Stefan-Boltzmann constant

*Subscripts*

$e$ = edge of the freestream
$j$ = species label
$s$ = solid
0 = surface
1 = glowing combustion
2 = flaming combustion

## Introduction

RADIOISOTOPE thermoelectric generators have become a conventional source of electrical power for spacecraft (e.g., in the past, Voyager; currently, Galileo and Ulysses). The thermal energy input for this power conversion process is typically provided through the nuclear decay of plutonia fuel. For obvious safety reasons, the fuel inventory is packaged and sealed in modular assemblies termed heat soures that are required to act as re-entry bodies in the event of a mission accident yielding an Earth return.

One design feature is the use of an outer enclosure to serve as a heat shield against the hostile thermal environments encountered during passage through a re-entry heat pulse. Bulk graphite materials such as the ATJ and POCO grades were used in the earlier heat sources, while the more advanced three-dimensional carbon/carbon material systems are used in the current-generation designs (e.g., the General-Purpose Heat Source for Galileo and Ulysses). Perhaps a more obscure re-entry design feature is the provision of a low ballistic coefficient design through judicious selection of materials and geometry. This feature serves a vital safety function by reducing terminal velocity to levels that substantially lower the risk of containment rupture and subsequent fuel release into the local environment upon impact.

The preceding design strategy gives rise to a class of re-entries characterized by long flight periods in the combined low-supersonic and subsonic velocity regimes; thus oxidation of the carbon heat shield becomes an important design consideration. Sizing of the heat shield must clearly account for oxidation mass loss during this long flight period. However, a more subtle ramification is the contribution of the carbon oxidation process in establishing the energy balance boundary condition which determines the interior thermal response of the heat source assembly. The eventual impact temperature of the interior fuel clad member influences its ability to arrest impact energies without rupture.

Recognizing this role for oxidation, and further understanding that numerous re-entry analyses are required in assessing a design's safety performance, there is clearly a need for an engineering predictive model for carbon oxidation that is rational and self-consistent yet computationally efficient. This paper proposes such a model and will demonstrate the importance of nonequilibrium chemistry on impact temperatures through a variety of sample problems.

The chemical model agrees reasonably well with experimental data[1] on the ablation rate of carbon in air at relatively low surface tempertures (i.e., below 1800 K). Heat source surface temperatures typically decay into this range during the low-supersonic and subsonic reaches of flight. Two sets of chemical reactions are written to correspond to the two basic modes of burning, namely glowing and flaming combustion. Glowing combustion is the simpler mode. Here the important reaction occurring at the local surface is

$$2C(s) + O_2(g) \rightarrow 2CO(g) \quad (1)$$

in which $s$ and $g$ denote solid and gaseous physical states.

The chemical mechanism of flaming combustion involves two reactions coupled to form a feedback loop:

$$C(s) + CO_2(g) \rightarrow 2CO(g) \quad (2)$$

$$2CO(g) + O_2(g) \rightarrow 2CO_2(g) \quad (3)$$

The gas phase reaction [Eq. (3)] generates $CO_2$, some of which diffuses back to the surface where it reacts with carbon to supply the necessary CO in reaction (2). Reaction (3) physically represents a detached flame.

The solution of these equations provides both the heat-shield mass flux loss and the associated surface energy contribution due to carbon oxidation kinetics. For purposes of il-

Presented as Paper 85-0904 at the AIAA 20th Thermophysics Conference, Williamsburg, VA, June 19-21, 1985; revision received Jan. 30, 1986. 

*Chemist.
†Mechanical Engineer.
‡Aerospace Engineer.
§Aerothermal Design Engineer.

lustration, the proposed oxidation model was applied as boundary conditions in a calculation of the recession and surface temperature as functions of altitude for a representative heat source design on a typical trajectory. These results are compared to more restrictive diffusion-limited calculations to further illustrate the importance of finite rate chemistry on heat source re-entry performance.

## Glowing Combustion

In performing these calculations, boundary-layer transport was simplified by assuming mass diffusivity for all species equal and equivalent to thermal diffusivity (i.e., Lewis number = 1). The notation of Kays[2] is followed as far as possible in describing the mass-transfer processes and the resulting energy boundary condition.

In very dry air (less than 10 ppm of $H_2O$ by mass[3]) and in humid air at sufficiently low temperatures (to be discussed below) the mechanism is glowing combustion, Eq. (1). Direct formation of $CO_2$ is relatively much slower[4] and, therefore, is neglected. The rate coefficient is denoted $k_1$ and depends on surface temperature through an Arrhenius law of the form

$$k_1 = A_1 e^{-E_1/T} \tag{4}$$

where $A_1$ and $E_1$ are constants. The rate coefficient determines the net species mass fluxes at the surface ($y=0$) due to convection and diffusion, as follows:

$$\dot{m}''(m_{CO})_0 - \rho D\left(\frac{dm_{CO}}{dy}\right)_0 = 2M_{CO}k_1\rho\frac{(m_{O_2})_0}{M_{O_2}} \tag{5}$$

$$\dot{m}''(m_{O_2})_0 - \rho D\left(\frac{dm_{O_2}}{dy}\right)_0 = -M_{O_2}k_1\rho\frac{(m_{O_2})_0}{M_{O_2}} \tag{6}$$

$$\dot{m}''(m_{N_2})_0 - \rho D\left(\frac{dm_{N_2}}{dy}\right)_0 = 0 \tag{7}$$

In these equations $\dot{m}''$ is the mass flux into the gas phase, $m_j$ the mass fraction of species $j$, $M_j$ the molecular weight of species $j$, $\rho$ the densitity, $D$ the mass diffusivity, and $y$ the distance from the surface.

These equations may be inverted to get $\dot{m}''$ and the species concentrations. To do so the derivatives are eliminated in favor of the concentrations at the edge of the boundary layer

$$\rho D\left(\frac{dm_j}{dy}\right)_0 = [(m_j)_e - (m_j)_0]\frac{\dot{m}''}{B} \tag{8}$$

where the mass-transfer parameter[2] $B$ has been assumed to satisfy

$$\dot{m}'' = g^* \ell n(1+B) \tag{9}$$

and $g^*$ is the mass-transfer conductance in the limit of no blowing. Equations (5-7) may then be solved to give the following concentrations:

$$(m_{CO}) = \frac{(m_{CO})_e + (M_{CO}/M_C)B_1}{1+B_1} \tag{10}$$

$$(m_{O_2})_0 = \frac{(m_{O_2})_e - (M_O/M_C)B_1}{1+B_1} \tag{11}$$

$$(m_{N_2})_0 = \frac{(m_{N_2})_e}{1+B_1} \tag{12}$$

along with an implicit equation for $\dot{m}''$ which may be inverted approximately to give

$$\dot{m}'' = g^*(1+Da_1^{-1})^{-1}\ell n\left[1+\frac{M_C}{M_O}(m_{O_2})_e\right] \tag{13}$$

where $Da_1$ is the Damköhler number

$$Da_1 = k_1\rho/g^* \tag{14}$$

The subscript 1 on $B$ and $Da$ corresponds to the rate coefficient $k_1$ and denotes the glowing combustion mechanism.

In examining Eq. (13), it is noted that the Damköhler number compares the rate coefficient $k_1$ to a characteristic speed $g^*/\rho$, at which $O_2$ is supplied to the surface. At low temperatures $k_1$ is small, and hence $\dot{m}''$ becomes small and controlled by temperature. However, at high temperatures $Da_1$ is large and $\dot{m}''$ becomes independent of $Da_1$. For this condition, Eq. (13) reduces to the usual diffusion-limited result.

The concentrations may be used to evaluate the specific enthalpy $i$ of the gas mixture at the surface, the value of which is necessary in determination of the net heat flux conducted into the interior, $\dot{q}''$. The typical re-entry energy boundary condition may be stated as

$$\dot{q}'' = \dot{m}''(i_0 - i_{s0}) + \frac{\dot{m}''}{B}(i_e - i_0) + I - \epsilon\sigma T^4 \tag{15}$$

Here $i_{s0}$ is the enthalpy per unit mass of the carbon at the surface, $I$ the incident radiation flux, and $\epsilon\sigma T^4$ the reradiation. The result is

$$\dot{q}'' = g\sum_j (m_j)_e[(i_j)_e - (i_j)_0] - \frac{\dot{m}''}{M_c}(\Delta\bar{i})_1 + I - \epsilon\sigma T^4 \tag{16}$$

in which

$$g = \dot{m}''/B \tag{17}$$

where $i_j$ is the partial enthalpy of species $j$ per unit mass and $(\Delta\bar{i})_1$ is the change in partial molar enthalpy for reaction (1). Thus the first term contains the sensible enthalpy drop between the freestream and the surface without chemical reactions, while the second term accounts for the heat of reaction. The quantity $g$ is equated to an enthalpy-based heat-transfer coefficient under the unity Lewis number assumption. In the limit of no blowing ($\dot{m}''\to 0$), $g$ reduces to $g^*$.

## Flaming Combustion

A similar calculation may be made for the flaming mechanism. The species concentrations at the surface are

$$(m_{CO})_0 = \frac{(2M_{CO}/M_C)B_2 - (M_{CO}/M_O)(m_{O_2})_e + (m_{CO})_e}{1+B_2} \tag{18}$$

$$(m_{CO_2})_0 = \frac{(m_{CO_2})_e + (M_{CO_2}/M_O)(m_{O_2})_e - (M_{CO_2}/M_C)B_2}{1+B_2} \tag{19}$$

$$(m_{N_2})_0 = \frac{(m_{N_2})_e}{1+B_2} \tag{20}$$

The form of the mass flux is the same as for the glowing mechanism:

$$\dot{m} = g^*(1+Da_2^{-1})^{-1}\ell n\left[1+\frac{M_C}{M_O}(m_{O_2})_e\right] \tag{21}$$

where now

$$Da = k_2\rho/g^*, \quad k_2 = A_2 e^{-E_2/T} \tag{22}$$

and the subscript 2 on $Da$ and $B$ denotes flaming combustion parameters. The heat flux includes the sensible enthalpy drop

and terms for the heats of reactions (2) and (3):

$$\dot{q}'' = g \sum_j (m_j)_e (i_{je} - i_{j0}) - g\frac{(\Delta\bar{i})_3}{2M_O}(m_{O_2})_e$$

$$-\dot{m}''\frac{(\Delta\bar{i})_2}{M_C} + I - \epsilon\sigma T^4 \tag{23}$$

The formula for $(m_{CO})_0$ leads to the requirement that

$$B_2 \geq \frac{M_C}{2M_O}(m_{O_2})_e - \frac{M_C}{2M_{CO}}(m_{CO})_e \tag{24}$$

which translates to

$$Da_2 \geq 1.082 \tag{25}$$

Equality is achieved when the mass fraction of CO at the surface drops to 0, corresponding to flame attachment.[5] This sets a lower limit on the temperature at which the simple flaming mechanism can provide a self-consistent description of carbon combustion. At lower temperatures the surface reaction is unable to generate CO fast enough to support a detached flame.

It is also important to note that the oxidation of CO by reaction (3) is possible only when enough $H_2O$ vapor is present —the $H_2O$ being a necessary catalyst for the reaction. As a first estimate, the relative humidity should exceed 0.1% (Ref. 3), which equates to an atmospheric altitude of about 12 km or lower. Thus, for purposes of modeling, a spacecraft reentering the Earth's atmosphere cannot experience flaming combustion until it has penetrated the 12-km threshold.

## Comparison with Experiment

This section compares the calculated mass flux with measurements by Matsui et al.[1] for carbon burning in air at $10^5$ Pa pressure. The experiments were run at surface temperatures from 1000 to 1800 K to show the transition from a kinetic controlled process to a diffusion-controlled process.

The measurements were made in axisymmetric, incompressible stagnation flow at controlled velocity gradients. The B-number for the flow was calculated by Tsuji and Matsui (see Ref. 5, Fig. 2). Their results may be approximately represented by Eq. (9) with a limiting conductance

$$g^* = 0.225 \text{ mg cm}^{-3} \times (2a \times 1.0 \text{ cm}^2 \text{ s}^{-1})^{1/2} \tag{26}$$

where $2a$ is the stagnation velocity gradient.

The activation temperatures of the two heterogeneous reactions for glowing and flaming combustion have been directly measured:[3]

$$E_1 = 2.65 \times 10^4 \text{ K} \tag{27}$$

$$E_2 = 4.0 \times 10^4 \text{ K} \tag{28}$$

The pre-exponential factors $A_1$ and $A_2$ in Eqs. (4) and (22) are not known to any accuracy; therefore, they were adjusted to give optimum agreement with experiment:

$$A_1 = 2.0 \times 10^{10} \text{ cm s}^{-1} \tag{29}$$

$$A_2 = 3.2 \times 10^{14} \text{ cm s}^{-1} \tag{30}$$

Figures 1-3 show the experimental data and superimposed calculations for glowing combustion (solid lines) and flaming combustion (dashed lines) in normal 293 K air at sea level. The velocity gradient in Figs. 1-3 characterizes the flow velocity field at the stagnation point. (In the case of spacecraft reentry, the velocity gradient reflects the shape and speed of the re-entry body. As an example, a body having a spherical radius of 30 cm and moving at terminal velocity in 293 K air at sea level experiences a velocity gradient of 1800 $s^{-1}$. In general, the velocity gradient is proportional to velocity and inversely proportional to an effective radius.[6])

At the higher temperatures shown in Figs. 1-3, the ablation rates for flaming and glowing combustion are indistinguishable. As temperature drops the two rates begin to separate, but flaming combustion stops before the difference gets very large. Since the humidity level in the experiments was large enough to permit flaming combustion, the predicted combustion rate follows the dashed curves at high temperatures and the solid curves at low temperatures. The predicted transition jump between the two mechanisms lies within the experimental scatter. In related experiments,[7] the humidity level was lowered to reduce the extent of flaming combustion. The ablation rate of from 1200 to 1400 K was observed to increase in agreement with the theory.

The accuracy of Eqs. (29) and (30) deserves some discussion. The predicted glowing mass flux, Eq. (13), is proportional to $A_1$ below 1200 K. Given the constraint that all of the solid curves in Figs. 1-3 use the same value of $A_1$, the choice of $A_1$ is limited to about ±10%. The agreement with experiment is very good in Figs. 2 and 3, but less favorable in Fig. 1. Based on Fig. 1, a pessimistic estimate of the accuracy is taken to be within a factor of 2. The flaming curves (dashed lines) are less sensitive to $A_2$ since the curves stop in the middle of the transition region. The values of $A_1$ and $A_2$ given in Eqs. (29) and

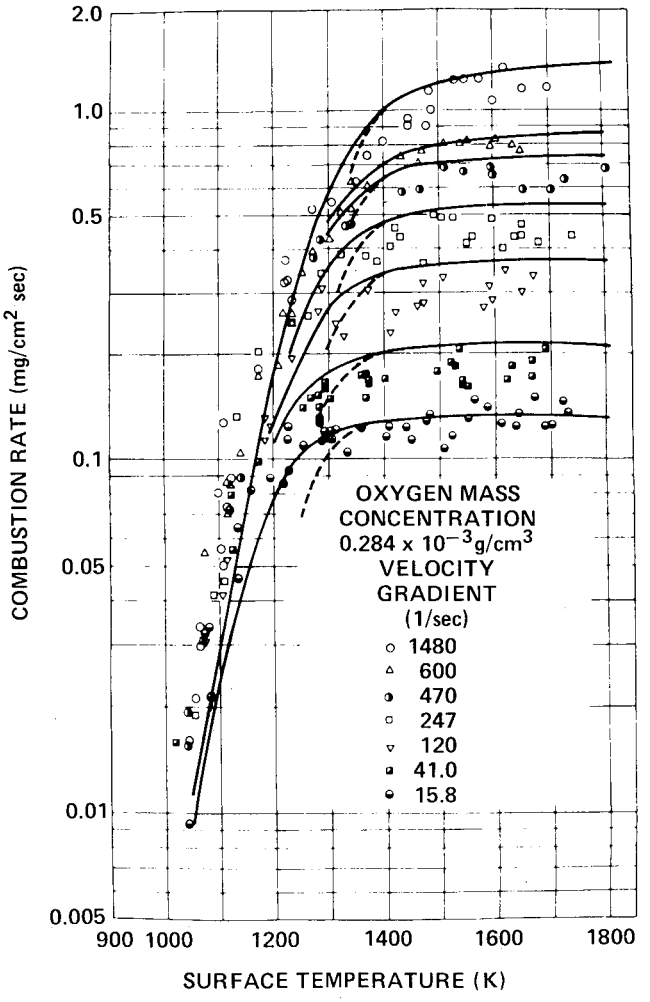


**Fig. 1 Carbon ablation rate measurements from Ref. 1 with calculated curves superimposed. The solid curves are calculated for the glowing combustion mechanism, and the dashed curves are for flaming combustion. The velocity gradient is varied at a fixed $O_2$ level.**

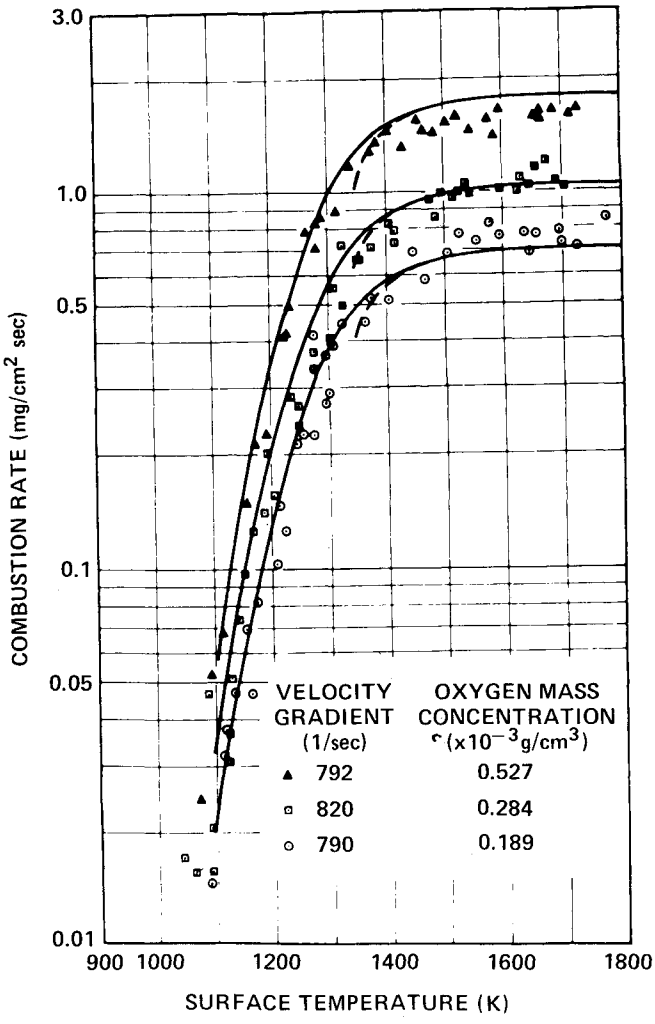


**Fig. 2 Calculated ablation rates compared with measurements from Ref. 1. The $O_2$ level is varied at a fixed velocity gradient.**

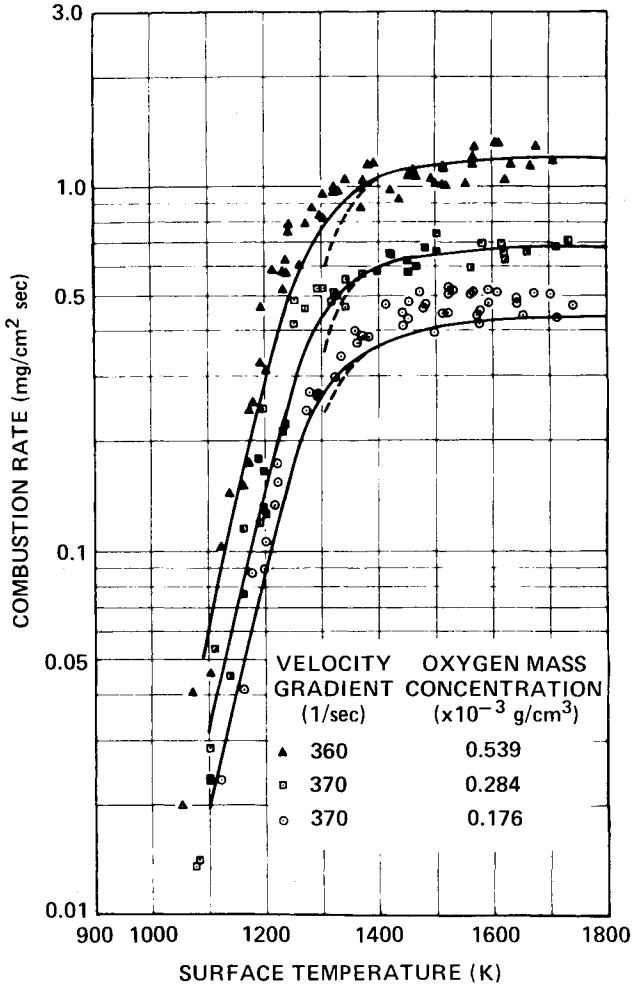


**Fig. 3 Calculated ablation rates compared with Ref. 1. The $O_2$ level is varied at a fixed velocity gradient.**

(30) are similar in magnitude to the pre-exponential factors observed for evaporation rates.[8]

## Re-Entry Calculations

This section illustrates the effect of finite-rate chemistry on ablation and thermal performance of a low ballistic coefficient re-entry body. Specifically, attention is directed toward the heat-shield performance of a solitary General-Purpose Heat Source (GPHS) module.

Briefly, the GPHS represents the thermal energy source of the radioisotope thermoelectric generator systems used to electrically power the Galileo and Ulysses spacecraft. The heat source has been designed as a universal modular assembly wherein each module delivers 250 thermal Watts of energy via the decay of plutonia fuel. The modules are arrayed in tandem within a converter housing to meet the power requirements of a particular mission.

The outer envelope of the module's heat shield is a parallelepiped with dimensions of $9.7 \times 9.3 \times 5.3$ cm. The heat shield is fabricated from a three-dimensional carbon/carbon material and has a minimum wall thickness of 4.8 mm at the module's broad face. To illustrate the chemistry effect, calculations were restricted to a one-dimensional stagnation heating thermal analysis with the parameters of interest being the heat shield's thermochemical recession and surface temperature response. The module was assumed to maintain a fixed aerodynamic trim orientation defined by its broad face normal to the velocity vector throughout the re-entry flight period.

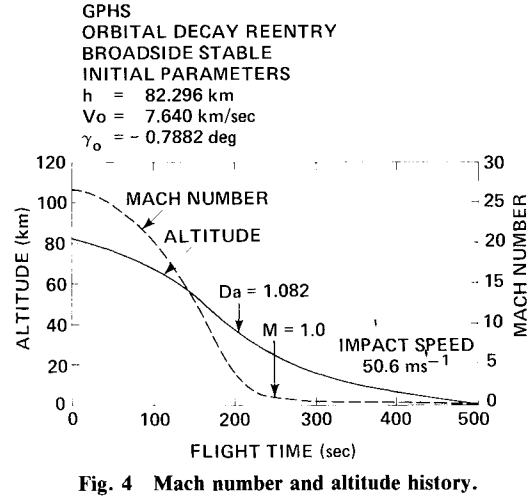


**Fig. 4 Mach number and altitude history.**

The trajectory chosen for these calculations was based on an orbital decay re-entry, which is the most probable type of re-entry according to the probabilistic failure mode and effects analysis conducted as part of a mission's overall safety analysis (e.g., Ref. 9). The orbital decay trajectory resulting from a three-degree-of-freedom flight simulation[10] is shown in Fig. 4. It is noted that the total flight period is about 500 s, with equal dwell time in the supersonic and subsonic velocity regimes. Given this trajectory information, available GPHS module experimenal heating rate data and standard stagnation

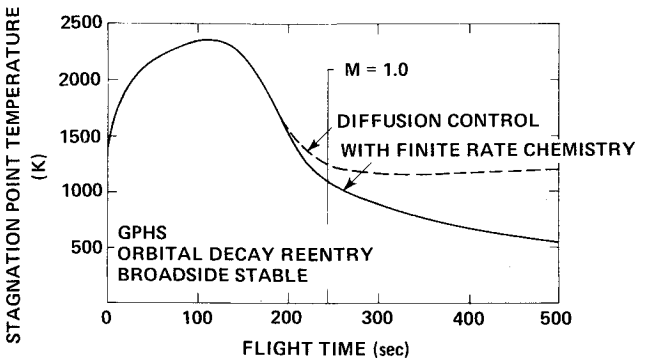


**Fig. 5 Stagnation point temperature history.**

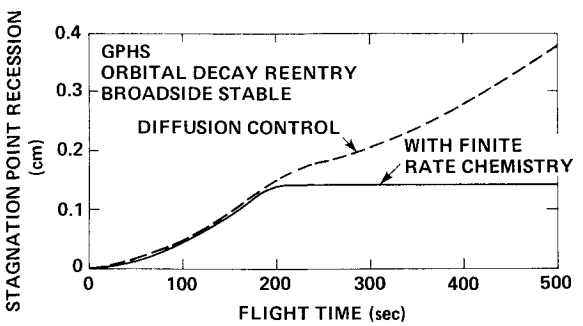


**Fig. 6 Recession history.**

heating rate correlations[11] were used to provide histories of the total freestream enthalpies, the stagnation $g^*$, and the relationship between the stagnation mass flux and the mass-transfer parameter.

From the preceding methodology, the mass flux and heat flux can now be calculated by formulas given in the preceding sections. The choice of glowing vs flaming combustion is made on the basis of both altitude (i.e., humidity) and $Da_2$ (which controls flame attachment). The equilibrium limits were obtained by dropping the Damköhler factors in the mass fluxes. Calculations were performed using an abridged version of an AEROTHERM code[12,13] which was further modified to accept the boundary conditions developed here. It is noted that the analysis included proper thermal ballast to represent the module's interior fuel containment assembly.

Figure 5 shows the effect of finite rate chemistry on heat-shield stagnation surface temperatures. Departure from the diffusion limit begins while the speed is still supersonic. By impact, a difference of over 500 K is obtained. The Damköhler number $Da_2$ exceeds 1.082 (the condition for a detached flame) only at altitudes above about 40 km, where the humidity level is too low to catalyze flaming. Thus flaming combustion is not achieved during this re-entry.

Figure 6 shows the heat-shield stagnation recession. Here the difference between the finite rate and equilibrium calculations is even more dramatic. By impact the equilibrium prediction is more than double the finite rate prediction. The additional recession is over 2 mm, most of which occurs during subsonic flight when the finite rate model predicts negligible amounts.

Thus these calculations, while somewhat simplified for design purposes, point to the importance of finite-rate chemistry in carbon ablation calculations for low ballistic coefficient trajectories.

## Conclusions

An engineering model for predicting finite rate carbon oxidation has been presented, which is self-consistent and computationally efficient. The model recognizes two oxidation processes, namely, glowing combustion and flaming combustion, and provides criteria in terms of relative humidity and a Damköhler number to differentiate between the two mechanisms. The model has been demonstrated to successfully predict carbon mass loss rates measured by Matsui et al.[1]

A reliable finite-rate carbon oxidation model has an important role in carbon heat-shield design for low ballistic coefficient re-entry bodies. A particular application relates to the re-entry safety design of a radioisotope heat source. The importance of the oxidation model was illustrated by examining the heat-shield response of a General-Purpose Heat Source module for an orbital decay re-entry condition. Approximately one-half of the total flight time for this re-entry resides in the low-supersonic/subsonic velocity regime where carbon ablation is largely governed by finite-rate oxidation. Results of this analysis clearly indicate the decisive effect of the subject finite-rate chemistry model in predicing heat-shield recession and thermal response.

## Acknowledgments

This work was sponsored by the U.S. Department of Energy office of Special Nuclear Projects, and the Naval Sea Systems Command (IRAD) under Contract N00024-85-C-5301. The authors wish to thank J.C. Hagan of the Johns Hopkins University/Applied Physics Laboratory for his encouragement and suggestions.

## References

[1]Matsui, K., Kôyama, A., and Uehara, K., "Fluid-Mechanical Effects on the Combustion Rate of Solid Carbon," *Combustion and Flame,* Vol. 25, 1975, p. 57.

[2]Kays, W.M., *Convective Heat and Mass Transfer,* McGraw-Hill Book Co., New York, 1966.

[3]Adomeit, G., Mohiuddin, G., and Peters, N., "Boundary Layer Combustion of Carbon," *Sixteenth Symposium (International) on Combustion,* The Combustion Institute, Pittsburg, PA, 1977, p. 731.

[4]Arthur, J.R., "Reactions Between Carbon and Oxygen," *Transactions of the Faraday Society,* Vol. 47, 1951, p. 164.

[5]Tsuiji, H. and Matsui, K., "An Aerothermochemical Analysis of Combustion of Carbon in the Stagnation Flow," *Combustion and Flame,* Vol. 26, 1976, pp. 283-297.

[6]Perini, L.L., "Laminar Heat Transfer Distribution Around Spheres and Cylinders in Subsonic-Supersonic Flow," Aerospace Nuclear Safety Program, The Johns Hopkins Univesity/Applied Physics Laboatory, Laurel, MD, Rept. ANSP-098, May 1977.

[7]Matsui, K., Tsuiji, H., and Makino, A., "The Effects of Water Vapor Concentration on the Rate of Combustion of an Artificial Graphite in Humid Air Flow," *Combustion and Flame,* Vol. 50, 1983, p. 107.

[8]Dushman, S. and Lafferty, J.M., *Scientific Foundations of Vacuum Technique,* John Wiley & Sons, New York, 1962.

[9]"Updated Safety Analysis Report for the Galileo Mission and the International Solar-Polar Mission," Advanced Energy Programs Department, General Electric Co., Valley Forge, PA, Doc. GESP-7186, April 1984.

[10]Perini, L.L., "Users Manual for the 3 DOF Trajectory Computer Program," Aerospace Nuclear Safety Program, The Johns Hopkins University/Applied Physics Laboratory, Laurel, MD Rept. ANSP-M-6, Sept. 1973.

[11]Conn, D.W., "GPHS Aerothermodynamic and Ablation Methodology," Aerospace Nuclear Safety Program, the Johns Hopkins University/Applied Physics Laboratory, Laurel, MD, Rept. ANSP-244, Sept. 1973.

[12]"Aerotherm Charring Material Thermal Response and Ablation Program (CMA)," AFRPL-TR-70-92, April 1970.

[13]"Aerotherm Equilibrium Surface Thermochemistry Computer Program (EST)," AFRPL-TR-70-93 April 1970.